JOURNAL OF AGRICULTURAL AND FOOD CHEMISTRY

# Atrazine Photodegradation in Aqueous Solution Induced by Interaction of Humic Acids and Iron: Photoformation of Iron(II) and Hydrogen Peroxide

XIAOXIA OU, XIE QUAN,* SHUO CHEN, HUIMIN ZHAO, AND YAOBIN ZHANG

Key Laboratory of Industrial Ecology and Environmental Engineering, Ministry of Education. School of Environmental and Biological Science and Technology, Dalian University of Technology, Dalian, China, 116024

The photochemical formation of Fe(II) and hydrogen peroxide ($H_2O_2$) coupled with humic acids (HA) was studied to understand the significance of iron cycling in the photodegradation of atrazine under simulated sunlight. The presence of HA significantly enhanced the formation of Fe(II) and $H_2O_2$, and their subsequent product, hydroxyl radical ($^{\bullet}OH$), was the main oxidant responsible for the atrazine photodegradation. During 60 h of irradiation, the fraction of iron presented as Fe(II) (Fe(II)/Fe(t)) decreased from 20–32% in the presence of the Fe(III)–HA complex to 10–22% after adding atrazine. The rate of atrazine photodegradation in solutions containing Fe(III) increased with increasing HA concentration, suggesting that the complexation of Fe(III) with HA accelerated the Fe(III)/Fe(II) cycling. Using fluorescence spectrometry, the quenching constant and the percentage of fluorophores participating in the complexation of HA with Fe(III) were estimated by the modified Stern–Volmer equation. Fourier transform infrared spectroscopy (FTIR) offered the direct evidence that Fe(III)–carboxylate complex could be formed by ligand exchange of HA with Fe(III). Based on all the information, a possible reaction mechanism was proposed.

**KEYWORDS: Humic acid; iron; hydrogen peroxide; hydroxyl radical; atrazine; photodegradation**

## INTRODUCTION

Iron plays a crucial role in many significant chemical and biological processes in natural waters where it occurs in dissolved and particulate forms (*1*). Iron cycling between ferrous and ferric species is also important for a number of reasons. First, iron may limit the growth of various biota including phytoplankton in the euphotic zone of surface waters because of its role as a micronutrient (*2*). Second, the Fe(II)–Fe(III) cycle is involved in many redox reactions, including the decomposition of $H_2O_2$ (*3*), the conversion of S(IV) to S(VI) (*4, 5*), and the redox cycling of trace metals such as Cr(III)/Cr(VI) (*6, 7*) and As(III)/As(V) (*8*) in natural waters. While these processes are always accompanied by the formation and consumption of active species (e.g. $^{\bullet}OH$, $^1O_2$, $ROO^{\bullet}$, and $HO_2^{\bullet}/O_2^{\bullet-}$) (*3, 9*), so the oxidizing capacity of the natural waters is influenced significantly by the iron cycling. Finally, because of their complex interaction, iron cycling is known to catalyze the oxidation of natural organic matter (NOM) in aquatic systems (*10, 11*) and, therefore, may play an important role in the global carbon cycle.

In the aquatic environment, humic acids (HA), the major constituents of the NOM, have complexing and reducing abilities and thus could dominate the speciation of iron. Studies have shown that the rate of photochemical iron reduction was affected by the presence of organic compounds through the ligand-to-metal charge transfer (LMCT) reactions of their complex (*1, 12*). Barbeau et al. (*13*) reported the key features of the iron cycle involving photolysis of Fe(III)–ligand complexes, with reduction of Fe(III) to Fe(II) and oxidation of the ligand. The wavelength dependence and quantum yields of Fe(II) photoformation in aerosol particles have been studied, and the results had implications to daytime Fe(III)/Fe(II) cycles in the atmospheric liquid phase (*14*). Zhao et al. (*15*) observed a regular oscillation in the ratio of Fe(II) to total iron when dissolved organic matter (DOM) was periodically added into the solution under irradiation. Photochemical processes involving iron and DOM lead to the formation of Fe(II) and the decomposition of DOM. As a result, DOM could be photodecomposed to the low molecular weight (LMW) organic compounds or photomineralized to inorganic carbon (e.g. $CO_2$) (*16, 17*). In addition, the reaction of the oxidized DOM with oxygen could produce the reactive oxygen species (ROS) including $^1O_2$, $O_2^{\bullet-}$, $H_2O_2$, and $^{\bullet}OH$. These ROS will oxidize DOM and Fe(II), in turn, oxidize the persistent toxic substances (PTS) that coexist in the natural waters.

Atrazine (2-chloro-4-ethylamino-6-isopropylamino-1,3,5-triazine) is one of the most widely used agricultural herbicides and has been detected in groundwater and surface water due to its persistence (*18–20*). Atrazine has been extensively used

* Corresponding author. Tel.: +86-411-84706140; fax: +86-411-84706263; e-mail address: quanxie@dlut.edu.cn.

10.1021/jf0719050 CCC: $37.00 
Published on Web 09/25/2007

in the control of broadleaf and grass weeds, primarily on corn and sorghum crops (*21*). It is significant to investigate the environmental fate of atrazine in natural waters since it is a suspected endocrine disruptor (ED) and a possible human carcinogen.

Solar irradiation can initiate important transformation pathways of pollutants in surface waters containing sensitizers (e.g. NOM and nitrate) and metals (*22–24*). Many published studies on the photochemical redox reaction of Fe(III) complex of polycarboxylates indicated that the process was potentially important sources of Fe(II) and ROS in atmospheric water drops and surface waters (*25–27*). However, there is little information related to the role of iron photoredox cycling coupled with ROS on the phototransformation of pollutants in solutions containing Fe(III) and HA. A better understanding of indirect photodegradation of PTS by ROS generated by sunlight interacting with sensitizers will contribute to elucidating the potential photochemical process occurring in natural waters.

In this paper, we examined the photodegradation of atrazine in nearly neutral aqueous solutions containing HA and Fe(III) and the related mechanism was studied by investigating the iron redox chemistry and $H_2O_2$ formation during the process of atrazine photooxidation. With this study, we aim to get more insight into the photochemical degradation potential and mechanism of atrazine and related iron redox chemistry in aqueous solutions containing Fe(III) and HA, both of which are common constituents in the natural environment. To our knowledge, this is the first report on quantifying the photoformation of Fe(II) and $H_2O_2$ induced by the Fe(III)–HA complex during the long-term photodegradation of atrazine without aerating or adding chemical oxidants (e.g., $H_2O_2$).

## MATERIALS AND METHODS

**Standards and Reagents.** All chemicals were analytical reagent grade and used without further purification. Atrazine (AZ) was purchased from Sigma-Aldrich Chemical Company with a purity higher than 98%, and the stock solution was prepared by dissolving the required amount in methanol. Ferric ammonium sulfate, $NH_4Fe(SO_4)_2 \cdot 12H_2O$, was purchased from Shanghai Chemical Reagent Co. Ltd and was dissolved in an aqueous solution of 0.1 M $H_2SO_4$ as Fe(III) stock solution. All stock solutions were stored in a refrigerator at 4 °C in the dark and used within one month. Milli-Q water (resistivity ≥ 18 MΩ·cm) was used in all experiments.

**Humic Acids.** The powder of HA used here was isolated from broadleaf forest soils following the IHSS (International Humic Substance Society) procedures (*28*). The sample sites were situated in Heilongjiang province, China. The elemental composition of the obtained HA powder is 45.01% C, 4.12% H, 3.72% N, 46.27% O, and <1% ash (vario EL III, Elementar, Germany). The HA powder was dissolved in Milli-Q water that was adjusted by NaOH to pH 7.5–8.0, and this HA stock solution was stored in a refrigerator at 4 °C in the dark. The HA concentration was measured by a total organic carbon analyzer (TOC-$V_{CPH}$, Shimadzu, Japan).

**Procedure for Photochemical Experiments.** Irradiation of the aqueous solutions (200 mL) was carried out in a cylindrical reactor (its diameter is 6.0 cm and height is about 8.0 cm), equipped with a Xe lamp (Shanghai JiGuang Lighting Corporation, China) that was surrounded with a quartz jacket and the tap water cooling circuit maintained the solution temperature at 25 ± 1 °C. The Xe lamp in combination with a special glass filter restricting the transmission of wavelengths below 290 nm was used for sunlight simulation. An average irradiation intensity of ca. 35 mW/cm$^2$ was maintained throughout the experiments and was measured by a radiometer (model FZ-A, Photoelectric Instrument Factory Beijing Normal University, China). The Fe(III)–HA solutions were magnetically stirred for 1 h and the initial pH was adjusted at 6.1 ± 0.1 by 0.1 M HCl or NaOH before adding atrazine. The reaction solutions were always magnetically stirred during irradiation.

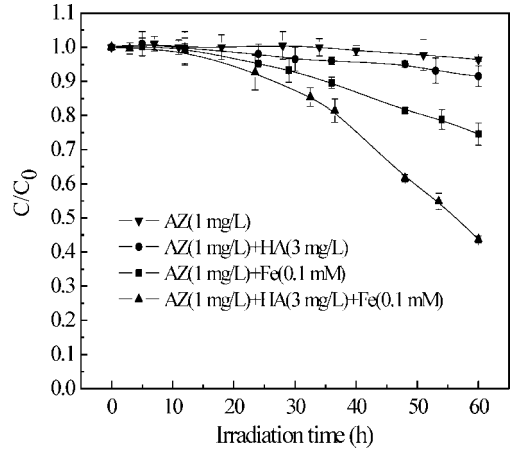


**Figure 1.** Photodegradation of atrazine as a function of time under Xe lamp ($\lambda$ > 290 nm) in different solutions at pH 6.1 ± 0.1.

**Chemical Analysis.** The concentration of atrazine was analyzed by HPLC (Waters-2695, PDA-2996, Waters, U.S.) equipped with a Kromasil ODS reverse-phase column (250 × 4.6 mm, 5.0 $\mu$m). Mixtures of methanol (55%) and water (45%) were used as the mobile phase at a flow rate of 1.0 mL/min and the detector wavelength was set at 220 nm. The concentration of Fe(II) and total iron (Fe(t)) were analyzed on a UV-vis spectrophotometer (UV-550, Jasco, Japan) using the 1,10-phenanthroline method. The concentration of total iron was almost unchanged under the experimental conditions. The absorbance was measured at 510 nm. A colorimetric method developed by Ghormley and co-workers (*29*) was used to measure $H_2O_2$ concentration in the reaction system. The $H_2O_2$ concentration was calculated by the absorbance of $I_3^-$ measured at 350 nm using a UV-vis spectrophotometer. The limit of detection for this method was around 10 nM.

**Characterization of Fe(III)–HA Complex.** The solutions of HA and Fe(III)–HA complex were stirred for 1 h in the dark to reach equilibrium. Their fluorescence was measured with 3D-EEM (excitation emission matrix) using a fluorescence spectrophotometer (model F-4500, Hitachi, Japan). The excitation wavelength ranged from 220 to 400 nm (5 nm bandwidth), and the emission from 250 to 550 nm (10 nm bandwidth). The sample preparation for Fourier-transform infrared spectra (FTIR) was carried out by mixing HA and Fe(III) with different concentrations, stirring for 6 h in the dark, followed by drying at ambient temperature and grinding to yield powder. Then 1 mg dry powdered sample was mixed with 100 mg KBr and measured by the FTIR spectrometer (Prestige-21, Shimadzu, Japan).

## RESULTS AND DISCUSSION

**Photochemical Degradation of Atrazine. Figure 1** showed the photodegradation of atrazine (1 mg/L) in different solutions at pH 6.1 under Xe lamp irradiation. No significant change over 60 h was observed in the atrazine alone solution, confirming that direct photodegradation initiated by wavelengths >290 nm can be ignored over the time scale considered. By addition of 3 mg/L HA, the concentration of atrazine decreased within 10%, and in the control experiment of 0.1 mM Fe(III), about 25% atrazine was degraded. In solution containing both HA and Fe(III), the obvious photodegradation was observed with 56.3% atrazine removal at the irradiation time of 60 h.

To see the mechanism responsible for atrazine photodegradation, the concentrations of Fe(II) and $H_2O_2$ formed in the different solutions were determined (**Figure 2**). In the system containing HA, $H_2O_2$ was produced through the reduction of oxygen by intermediates formed from excited

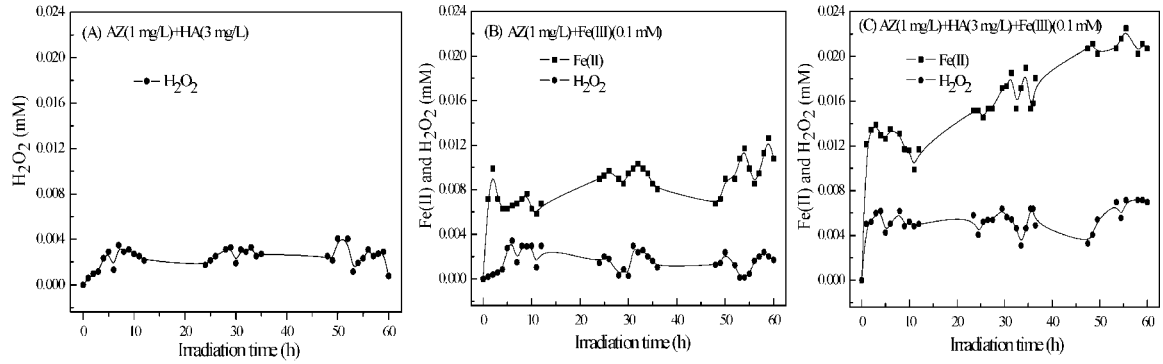


**Figure 2.** Formation and consumption of $H_2O_2$ and Fe(II) in different systems corresponding to Figure 1.

HA (eqs 1–3) and did not exceed 0.004 mM (**Figure 2A)**. Hence, $H_2O_2$ may be the oxidant responsible for the slight decrease of atrazine concentration.

$$HA + h\nu \rightarrow HA^* \quad (1)$$

$$HA^* + O_2 \rightarrow \text{Products} + O_2^{\bullet -}/HO_2^{\bullet} \quad (2)$$

$$O_2^{\bullet -}/HO_2^{\bullet} \rightarrow H_2O_2 \quad (3)$$

In iron control experiment, the explanation for the formation of Fe(II) (**Figure 2B)** was that a photoredox reaction occurred in which a hydroxide ion, bound in the inner-coordination sphere of a surface Fe(III) lattice atom (symbol: >Fe(III)), donated an electron to the excited lattice iron (*12, 30*):

$$>Fe^{III}(:OH^-) + h\nu \rightarrow >Fe^{III*}(:OH^-) \rightarrow >Fe(II) + {}^{\bullet}OH \quad (4)$$

Furthermore, $H_2O_2$ was produced in an iron control experiment from the disproportionation of superoxide ($O_2^{\bullet -}$) (eq 3), which was formed from the reduction of $O_2$ by Fe(II) (eq 5). The formed $H_2O_2$ can react with Fe(II) to generate $^{\bullet}OH$ (eq 6). Consequently, about 25% atrazine was degraded due to $^{\bullet}OH$ generated through the above two proposed pathways or more (eq 7).

$$Fe(II) + O_2 \rightarrow Fe(III) + O_2^{\bullet -}/HO_2^{\bullet} \quad (5)$$

$$Fe(II) + H_2O_2 \rightarrow Fe(III) + {}^{\bullet}OH + OH^- \quad (6)$$

$$\text{Atrazine} + {}^{\bullet}OH \rightarrow \text{Products} \quad (7)$$

As seen from **Figure 2C,** the Fe(II) and $H_2O_2$ concentrations were greatly enhanced due to the presence of HA. Absorption of a photon by an Fe(III)–HA complex initiated the yielding of Fe(II) and a free radical ($HA^{\bullet +}$) through LMCT within the complex (eq 8) and the follow-up reactions (eqs 2, 3, 5, 6, and 7) occurred. Following oxidation of Fe(II) by $O_2$ or $H_2O_2$, the resulting Fe(III) was reduced by HA, thus completing a reaction cycle. The iron cycling coupled with ROS cycle could be catalyzed by the presence of HA, and consequently, the rate of atrazine photodegradation was accelerated.

$$Fe(III)\text{–}HA + h\nu \rightarrow HA^{\bullet +} + Fe(II) \quad (8)$$

The results of Fe(II) and $H_2O_2$ measurements (**Figure 2**) are consistent with the results of atrazine photodegradation (**Figure 1**).

To further confirm that this decrease in atrazine concentration was caused by $^{\bullet}OH$, generated by reaction of Fe(II) and $H_2O_2$, experiments were conducted in solution containing HA and Fe(III) in the absence and presence of atrazine (**Figure 3**). The solution with HA and Fe(III), exhibited higher concentrations of Fe(II) and $H_2O_2$, especially for Fe(II), which was roughly

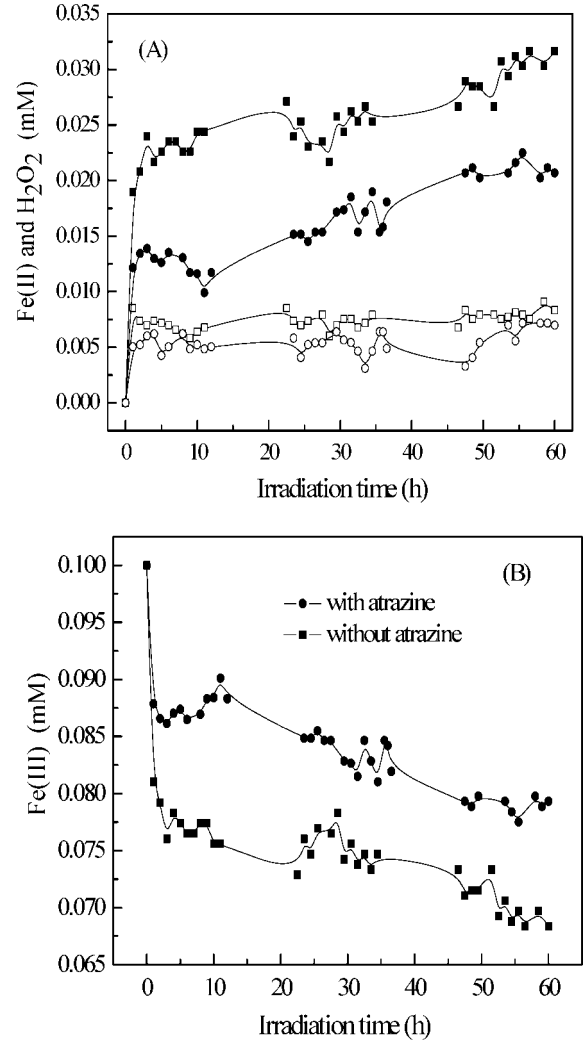


**Figure 3.** (**A**) Formation and consumption of Fe(II) and $H_2O_2$ in systems without atrazine (Fe(II), ■; $H_2O_2$, □) and with atrazine (Fe(II), ●; $H_2O_2$, ○). (**B**) Concentration of Fe(III). All systems initially contained 0.1 mM Fe(III) and 3 mg/L HA. In all the cases, the total iron concentration was 0.1 mM.

1.5 times of that observed in the solution containing atrazine, HA and Fe(III). Considering the iron cycle that consists of photoreduction of Fe(III) to Fe(II) by HA (eq 8) and subsequent oxidation of Fe(II) back to Fe(III) by $O_2$ or $H_2O_2$ (eqs 5 and 6), if the reaction rates of eqs 5 and 6 are slow compared to that of eq 8, a relatively high concentration of Fe(II) can be maintained (*11*). **Figure 3** displayed that when the atrazine was introduced into the binary system (Fe(III)/HA), the concentration of Fe(II) and $H_2O_2$ decreased sharply, inferring that reactions 5 and 6

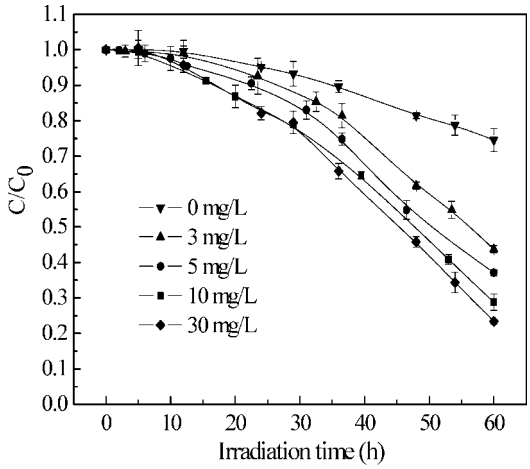


**Figure 4.** Effect of different initial HA concentrations (0, 3, 5, 10 and 30 mg/L) on atrazine degradation in systems containing 0.1 mM total iron and 1 mg/L atrazine at pH 6.1.

became faster due to the presence of atrazine. Specifically, atrazine reacted with •OH, which made the rates of eqs 5 and 6 become faster after adding atrazine. As a result, the amount of Fe(II) decreased and the Fe(III) concentration increased (**Figure 3A** and **B**). During 60 h of irradiation, the fraction of iron presented as Fe(II) (Fe(II)/Fe(t)) was 20–32% in the presence of Fe(III) and HA, and after adding atrazine, the Fe(II)/Fe(t) ratio decreased to 10–22%.

**Effect of HA Concentration on the Rate of Atrazine Photodegradation, and the Photoformation of Fe(II) and $H_2O_2$. Figure 4** showed the atrazine photodegradation at initial HA concentrations of 0, 3, 5, 10, and 30 mg/L at pH 6.1. The degradation rate of atrazine (initially 1 mg/L) in these irradiated systems containing 0.1 mM Fe(III), increased with increasing HA concentration. The atrazine degradation dependent on HA can be explained by the speciation of iron, a factor controlling the formation of •OH. It's well known that DOM, especially HA, have abilities to complex and reduce iron (*1*, *31*–*33*). Light-excited HA can effectively inject electrons into Fe(III) which leads to the production of Fe(II) and an easy cycle of Fe(III)/Fe(II) in the presence of $H_2O_2$ formed through eqs 2 and 3 and thus a continuous production of •OH. The generation of Fe(II) and $H_2O_2$ were in parallel to the depletion of HA and $O_2$. Apparently, more HA would increase the production of Fe(II) and $H_2O_2$.

**Figure 5** showed the photoformation of Fe(II) and $H_2O_2$ generated in Fe(III)–HA systems. As expected, with increasing HA concentration, the amounts of Fe(II) and $H_2O_2$ increased. At the end of irradiation (50–60 h), the Fe(II)/Fe(t) ratios were about 10, 23, 33, 44, and 90%, corresponding to 0, 3, 5, 10, and 30 mg/L HA, respectively, indicating that more HA are advantageous to Fe(II) photoformation.

However, the atrazine degradation in the presence of 30 mg/L HA was not enhanced significantly compared to that of 10 mg/L HA, which did not coincide with the results of Fe(II) and $H_2O_2$ photoformation in these two systems. The phenomenon could be possibly attributed to HA competing with atrazine for the available •OH. In the natural aquatic system, humic substances act as both source (when being a sensitizer) and sink (when being a quencher) of ROS, so the effects of HA on the photodegradation of the pollutant can be influenced by the amount of HA (*25*, *34*).

**Discussions on the Induction Period.** As can be seen from **Figure 4**, the concentration of atrazine changed slowly at beginning and then decreased fast. The rate of atrazine degradation was nearly constant after an induction period. The occurrence of induction period could be due either to the time needed for forming Fe(II) and $H_2O_2$, or to the binding interaction of atrazine and HA. In the system containing Fe(III)–HA complex, Fe(II) and $H_2O_2$ first have to be formed before the Fenton reaction (eq 6) can start to produce •OH that could oxidize atrazine effectively. As **Figure 5** showed, the Fe(II) and $H_2O_2$ concentrations indeed exhibited the trends of increasing. For example, at the HA concentration of 10 mg/L, the amount of Fe(II) formed at reaction beginning (1–12 h) was around 0.03 mM, while the Fe(II) produced in the end (50–60 h) was near 0.045 mM. On the other hand, binding of atrazine to HA through hydrophobic interaction (*35*, *36*) may have some negative effects on the photodegradation of atrazine. This hydrophobic binding mechanism draws the pollutant molecule into an aggregate of humic molecules (*34*), leading to that ROS generated in solution reacting with HA instead of atrazine. The hydrophobic groups of HA would be destroyed by absorption of photons during the irradiation, therefore, with increasing irradiation time the faster degradation of atrazine could occur as a result of the destroying the hydrophobic binding, which can inhibit atrazine photodegradation.

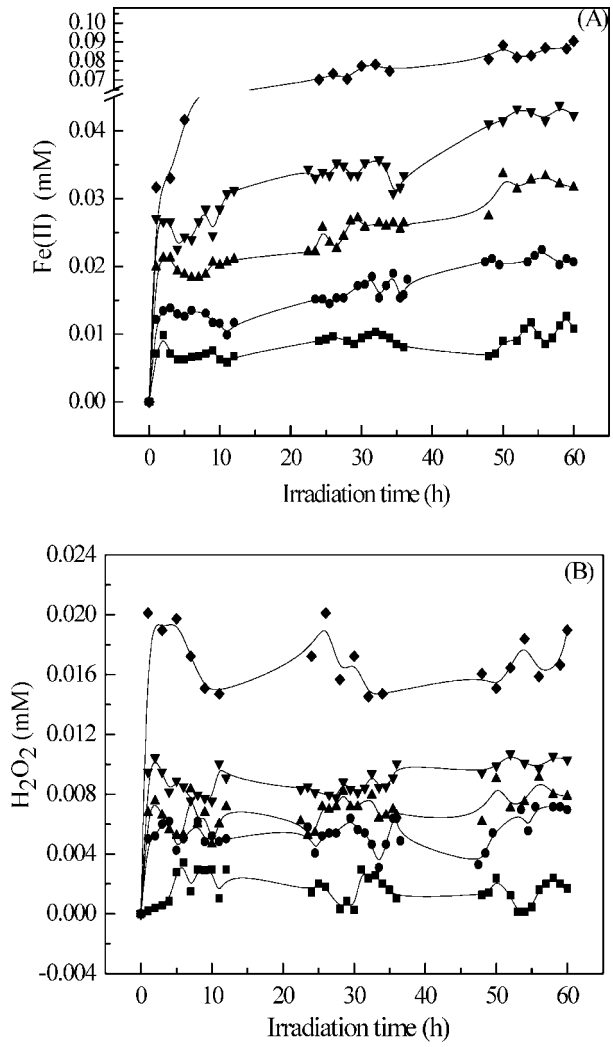


**Figure 5.** Formation and consumption of Fe(II) (**A**) and $H_2O_2$ (**B**) in different systems: 0 mg/L HA (■); 3 mg/L HA (●); 5 mg/L HA (▲); 10 mg/L HA (▼) and 30 mg/L HA (♦). All systems contained 0.1 mM Fe(III) and 1 mg/L atrazine.

**Fluorescence Quenching.** Fluorescence quenching titrations are often used to characterize binding properties. HA contain

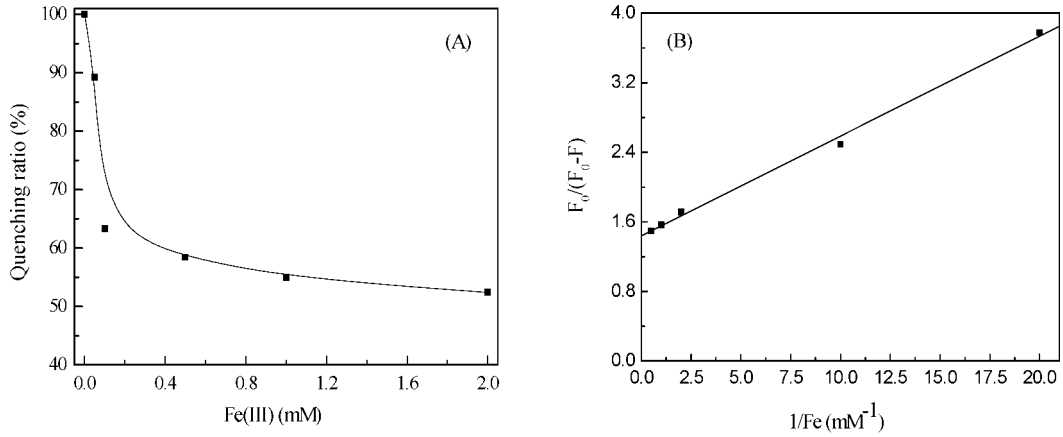


**Figure 6.** Fluorescence quenching of HA by Fe(III) at pH 6.1. (**A**) Iron quenching titration curve of HA. (**B**) Plot of the modified Stern-Volmer equation ($y = 0.1148\ x + 1.439$, $R^2 = 0.9967$). *x* and *y*-axis are referred to eq 9.

many fluorophores (*37*) and when metals are added in HA solution, a strong fluorescence quenching effect would be observed. **Figure 6A** gave the Fe(III) quenching titration curve of HA at 310/400 nm. As the amount of Fe(III) added in solution increased, the fluorescence intensity is decreased due to Fe(III) binding, and with the further addition of Fe(III), the fluorescence intensity of the system decreased gradually in the titration curve which indicated the beginning of saturation of the HA binding site.

The further quantitative analysis of the binding of Fe(III) to HA was carried out using the modified Stern–Volmer equation which was used to evaluate the complexing parameters, i.e. quenching constants and binding capacities (*38, 39*):

$$F_0/(F_0 - F) = 1/(fK_q[Q]) + 1/f \qquad (9)$$

where $F_0$ and $F$ are the fluorescence intensities in the absence and in the presence of quenchers, $K_q$ is the quenching constant, $f$ is the fraction of the initial fluorescence that corresponds to the binding fluorophores, and [Q] is the molar concentration of quencher. The modified Stern–Volmer plot for the quenching of HA fluorescence by Fe(III) was shown in **Figure 6B**. The results illustrated that the plot of $F_0/(F_0 - F)$ vs 1/[Q] is linear and the intercept of the straight line with the *y*-axis yields $f =$ 69%. The value of $K_q$ could be calculated from the slope ($1/fK_q$) and log $K_q$ of 4.10 was obtained. Esteves da Silva et al. (*40*) reported that the log $K_q$ and $f$ of fulvic acid (FA) samples extracted from composted sewage sludges quenched by Fe(III) at pH 4.0 were 4.87 and 90%, respectively, which are larger than our results. This can be attributed to a relatively higher percentage of fluorophores in FA compared to HA.

**FTIR Spectra.** FTIR spectra of HA were recorded with and without the addition of Fe(III) to investigate whether any structural change of HA occurred with the interaction of iron. **Figure 7a** was the FTIR spectra of HA, typical of those generally shown for humic substances extracted from soil, such as the bands at 3700–3200 $cm^{-1}$ for phenolic O–H stretching and at 1720-1700 $cm^{-1}$ for C=O stretching of –COOH (*41*). The spectra of the Fe(III)–HA complex (**Figure 7b**,**c**) showed changes in their bands as follows: (i) decreasing in the intensity of $\upsilon$(C=O) band of -COOH (▲, ~1714 $cm^{-1}$); (ii) increasing the bands assigned to the asymmetric and symmetric –COO– stretching (☆, ~1635 $cm^{-1}$ and △, ~1421 $cm^{-1}$). Furthermore, the higher variations in carboxylic and carboxylate bands were found in samples complexed with a greater amount of Fe(III). These observations indicated that a part of carboxylic acid in HA were deprotonated to form carboxylate by the ligand exchange with Fe(III) and the band at 1421 $cm^{-1}$ could be assigned to –COO–Fe. This assignment was in agreement with the result of Sposito (*42*) that a strong absorption band at about 1400 $cm^{-1}$ appeared when a soil fulvic acid interacted with Fe to form iron fulvate and complexed with goethite. It is believed that binding of iron and HA occurs predominantly through a ligand-exchange involving carboxylic functional groups of the HA and Fe(III).

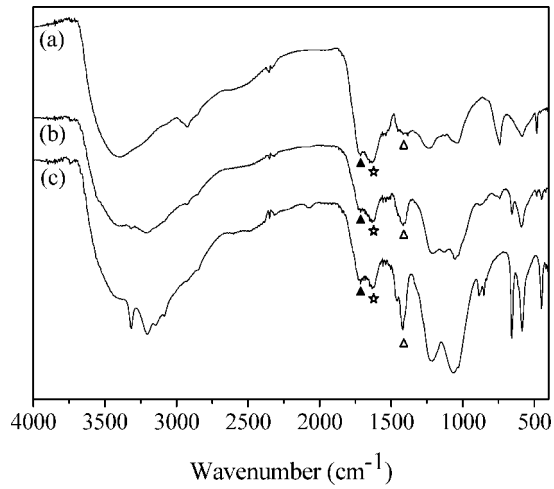


**Figure 7.** Comparison of FTIR spectra between HA and Fe(III)–HA complex. (**a**) HA(0.1 g), (**b**) HA(0.1 g) + Fe(III) (20 mM), (**c**) HA(0.1 g) + Fe(III) (60 mM).

**Mechanism Discussion.** On the basis of above discussions, a possible reaction mechanism in the presence of Fe(III)–HA complex was proposed in **Scheme 1**. When HA and Fe(III) coexist in solution, HA might react with iron species followed by the formation of iron–HA complexes, and photochemical reactions of these complexes take place by electron transfer from HA to the Fe(III) (LMCT) which could produce Fe(II) and consume HA. Then the reaction of the free humic radical with $O_2$ leads to $O_2^{\bullet-}/HO_2^{\bullet}$ formation, and $H_2O_2$ is the product of $O_2^{\bullet-}/HO_2^{\bullet}$ dismutation. Ultimately, the simultaneous and rapid photoformation of Fe(II) and $H_2O_2$ in the irradiated Fe(III)–HA system leads to $^{\bullet}OH$ formation. However, there are numerous concurrent processes in the systems, including the competing reactions of free HA radical ($HA^{\bullet+}$) with $O_2$ and Fe(III) species, and the $^{\bullet}OH$ quenched by both atrazine and HA. The net result was an iron redox cycle in which HA as well as oxygen were consumed, ROS were generated and reacted, and the degradation of atrazine was accelerated.

**Scheme 1.** Tthe Iron Cycling and Main Reactions in Fe(III)–HA Systems.

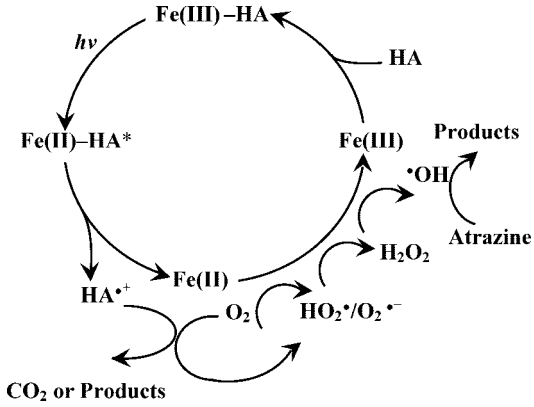


In summary, the Fe(III)–HA complex significantly increased the photodegradation rate of atrazine and the concentration of Fe(II) and $H_2O_2$ in nearly neutral aqueous solutions. The rate of atrazine photodegradation depended on the amount of •OH, being formed by reaction of Fe(II) and $H_2O_2$, which are likely to be higher at the higher concentration of HA. At a relatively high concentration, HA could act as a scavenger of •OH that are produced in the photo-Fenton reaction and hence compete with atrazine for •OH. Based on the characterization of Fe(III)–HA complex by fluorescence spectrophotometer and FTIR, the binding parameters were obtained and deprotonation of carboxylic acid of HA by the ligand exchange with iron was involved during the binding process. An iron redox cycle coupled with ROS depicted in **Scheme 1** should be a common phenomenon in natural waters, since both Fe(III) and humic substances are ubiquitous in the natural environment. This study is helpful in understanding the potential of toxic organic pollutants photodegradation in natural waters.

## LITERATURE CITED


(1) Voelker, B. M.; Morel, F. M. M.; Sulzberger, B. Iron redox cycling in surface waters: Effects of humic substances and light. *Environ. Sci. Technol.* **1997**, *31*, 1004–1011.

(2) Martin, J. H.; Fitzwater, S. E. Iron deficiency limits phytoplankton growth in the northeast Pacific subartic. *Nature* **1988**, *331*, 341–343.

(3) Zepp, R. G.; Faust, B. C.; Hoigne, J. Hydroxyl radical formation in aqueous reactions (pH 3-8) of iron(II) with hydrogen peroxide: the photo-Fenton reaction. *Environ. Sci. Technol.* **1992**, *26*, 313–319.

(4) Zhuang, G. S.; Zhen, Y.; Duce, R. A.; Brown, P. R. Link between iron and sulphur cycles suggested by detection of Fe(II) in remote marine aerosols. *Nature* **1992**, *355*, 537–539.

(5) Breytenbach, L. W.; Vanpareen, W.; Pienaar, J. J.; van Eldik, R. The role of organic acids and metal ions on the kinetics of the oxidation of S(IV) by hydrogen peroxide. *Atmos. Environ.* **1994**, *28*, 2451–2459.

(6) Hug, S. J.; Laubscher, H.-U. Iron(III) catalyzed photochemical reduction of chromium(VI) by oxalate and citrate in aqueous solutions. *Environ. Sci. Technol.* **1997**, *31* (1), 160–170.

(7) Gaberell, M.; Chin, Y.-P.; Hug, S. J.; Sulzberger, B. Role of dissolved organic matter composition on the photoreduction of Cr(VI) to Cr(III) in the presence of iron. *Environ. Sci. Technol.* **2003**, *37* (19), 4403–4409.

(8) Hug, S. J.; Leupin, O. Iron-catalyzed oxidation of arsenic(III) by oxygen and by hydrogen peroxide: pH-dependent formation of oxidants in the Fenton reaction. *Environ. Sci. Technol.* **2003**, *37* (12), 2734–2742.

(9) King, D. W.; Lounsbury, H. A.; Millero, F. J. Rates and mechanism of Fe(II) oxidation at nanomolar total iron concentrations. *Environ. Sci. Technol.* **1995**, *29*, 818–824.

(10) Voelker, B. M.; Sulzberger, B. Effects of fulvic acid on Fe(II) oxidation by hydrogen peroxide. *Environ. Sci. Technol.* **1996**, *30*, 1106–1114.

(11) Miles, C. J.; Brezonik, P. L. Oxygen consumption in humic-colored waters by photochemical ferrous-ferric catalytic cycle. *Environ. Sci. Technol.* **1981**, *15*, 1089–1095.

(12) David Waite, T.; Morel, F. M. M. Photoreductive dissolution of colloidal iron oxides in natural waters. *Environ. Sci. Technol.* **1984**, *18*, 860–868.

(13) Barbeau, K.; Rue, E. L.; Bruland, K. W.; Butler, A. Photochemical cycling of iron in the surface ocean mediated by microbial iron(III)-binding ligands. *Nature* **2001**, *413*, 409–413.

(14) Okada, K.; Kuroki, Y.; Nakama, Y.; Arakaki, T.; Tanahara, A. Wavelength dependence of Fe(II) photoformation in the water-soluble fraction of aerosols ccollected in Okinawa, Japan. *Environ. Sci. Technol.* **2006**, *40*, 7790–7795.

(15) Song, W. J.; Ma, W. H.; Ma, J. H.; Chen, C. C.; Zhao, J. C. Photochemical oscillation of Fe(II)/Fe(III) ratio induced by periodic flux of dissolved organic matter. *Environ. Sci. Technol.* **2005**, *39*, 3121–3127.

(16) Brinkmann, T.; Horsch, P.; Sartorius, D.; Frimmel, F. H. Photoformation of low-molecular-weight organic acids from brown water dissolved organic matter. *Environ. Sci. Technol.* **2003**, *37*, 4190–4198.

(17) Goldstone, J. V.; Pullin, M. J.; Bertilsson, S.; Voelker, B. M. Reactions of hydroxyl radical with humic substances: Bleaching, mineralization, and production of bioavailable carbon substances. *Environ. Sci. Technol.* **2002**, *36*, 364–372.

(18) Pionke, H. B.; Glotfelty, D. E.; Lucas, A. D.; Urban, J. B. Pesticide contamination of groundwaters in the Mahatango Creek watershed. *J. Environ. Qual.* **1988**, *17*, 76–84.

(19) Thurman, E. M.; Goolsby, D. A.; Meyer, M. T.; Mills, M. J.; Pomes, P. L.; Kolpin, D. W. A reconnaissance study of herbicides and their metabolites in surface water of the midwestern United States using immunoassay and gas chromatography/mass spectrometry. *Environ. Sci. Technol.* **1992**, *26*, 2440–2447.

(20) Evgenidou, E.; Fytianos, K. Photodegradation of triazine herbicides in aqueous solutions and natural water. *J. Agric. Food Chem.* **2002**, *50*, 6423–6427.

(21) Chu, W.; Chan, K. H.; Graham, N. J. D. Enhancement of ozone oxidation and its associated processes in the presence of surfactant: Degradation of atrazine. *Chemosphere* **2006**, *64*, 931–936.

(22) Vialaton, D.; Pilichowski, J.-F.; Baglio, D.; Paya-Perez, A.; Larsen, B.; Richard, C. Phototransformation of propiconazole in aqueous media. *J. Agric. Food Chem.* **2001**, *49*, 5377–5382.

(23) Latch, D. E.; McNeill, K. Microheterogeneity of singlet oxygen distributions in irradiated humic acid solutions. *Science* **2006**, *311*, 1743–1747.

(24) Larson, R. A.; Schlauch, M. B.; Marley, K. A. Ferric ion promoted photodecomposition of triazines. *J. Agric. Food Chem.* **1991**, *39*, 2057–2062.

(25) Faust, B. C.; Zepp, R. G. Photochemistry of aqueous iron(III)-polycarboxylate complexes: Role in the chemistry of atmospheric and surface waters. *Environ. Sci. Technol.* **1993**, *27*, 2517–2522.

(26) Zuo, Y.; Hoigne, J. Formation of hydrogen peroxide and depletion of oxalic acid in atmospheric water by photolysis of iron(III)-oxalato complexes. *Environ. Sci. Technol.* **1992**, *26*, 1014–1022.

(27) Zuo, Y. Kinetics of photochemical/chemical cycling of iron coupled with organic substances in cloud and fog droplets. *Geochim. Cosmochim. Acta* **1995**, *59*, 3123–3130.

(28) Swift, R. S. Organic matter characterization. In *Methods of Soil Analysis. Part 3. Chemical methods*; Sparks, D. L., Ed.; Soil Science Society of America: Madison, WI, 1996; pp 1018–1020.

(29) Allen, A. O.; Hochanadel, C. J.; Ghormley, J. A.; Davis, T. W. Decomposition of water and aqueous solutions under mixed fast neutron and gamma radiation. *J. Chem. Phys.* **1952**, *56*, 575–586.

(30) Cunningham, K. M.; Goidberg, M. C.; Weiner, E. R. Mechanisms for aqueous photolysis of adsorbed benzoate, oxalate, and succinate on iron oxyhydroxide (goethite) surfaces. *Environ. Sci. Technol.* **1988**, *22*, 1090–1097.

(31) Sonke, J. E. Lanthanide-humic substances complexation. II. Calibration of humic ion-binding model V. *Environ. Sci. Technol.* **2006**, *40*, 7481–7487.

(32) Chen, F.; Ma, W. H.; He, J. J.; Zhao, J. C. Fenton degradation of malachite green catalyzed by aromatic additives. *J. Phys. Chem. A* **2002**, *106*, 9485–9490.

(33) Bauer, M.; Heitmann, T.; Macalady, D. L.; Blodau, C. Electron transfer capacities and reaction kinetics of peat dissolved organic matter. *Environ. Sci. Technol.* **2007**, *41*, 139–145.

(34) Fu, H. B.; Quan, X.; Liu, Z. Y.; Chen, S. Photoinduced transformation of $\gamma$-HCH in the presence of dissolved organic matter and enhanced photoreactive activity of humate-coated $\gamma$-$Fe_2O_3$. *Langmuir* **2004**, *20*, 4867–4873.

(35) Piccolo, A.; Conte, P.; Scheunert, I.; Paci, M. Atrazine interactions with soil humic substances of different molecular structure. *J. Environ. Qual.* **1998**, *27*, 1324–1333.

(36) Schmitt, P.; Freitag, D.; Trapp, I.; Garrison, A. W.; Schiavon, M.; Kettrup, A. Binding of s-triazines to dissolved humic substances: electrophoretic approaches using affinity capillary electrophoresis (ACE) and micellar electrokinetic chromatography (MEKC). *Chemosphere* **1997**, *35*, 55–75.

(37) Hunt, J. F.; Ohno, T. Characterization of fresh and decomposed dissolved organic matter using excitation-emission matrix fluorescence spectroscopy and multiway analysis. *J. Agric. Food Chem.* **2007**, *55*, 2121–2128.

(38) Patel, A. B.; Srivastava, S.; Phadke, R. S. Interaction of 7-Hydroxy-8-(phenylazo)1,3-naphthalenedisulfonate with bovine plasma albumin. Spectroscopic studies. *J. Biol. Chem.* **1999**, *274*, 21755–21762.

(39) Lu, X. Q.; Jaffe, R. Interaction between Hg(II) and natural dissolved organic matter: a fluorescence spectroscopy based study. *Water Res.* **2001**, *35*, 1793–1803.

(40) Esteves da Silva, J. C. G.; Machado, A. A. S. C.; Oliveira, C. J. S. Fluorescence quenching of anthropogenic fulvic acids by Cu(II), Fe(III) and $UO_2^{2+}$. *Talanta* **1998**, *45*, 1155–1165.

(41) Schnitzer, M.; Khan, S. U. In *Humic Substances in the Environment*; Dekker: New York, 1972; pp 68–82.

(42) Sposito, G. *The Surface Chemistry of Soils*; Oxford University Press: New York, 1984.

**Received for review June 27, 2007. Revised manuscript received August 21, 2007. Accepted August 23, 2007. The work was supported by the National Natural Science Foundation (PR China, no. 20477005), the National Basic Research Program (PR China, no. 2004CB418504) and the National Science Foundation of Distinguished Young Scholars (PR China, no. 20525723).**

JF0719050